

The Surface Analysis of Niti Vertebral Implant Manufactured By Braiding Technique

Mahdis Parsafar

Department of Biomedical Engineering, Faculty of Paramedical Sciences, Tehran Medical Sciences, Islamic Azad University, Tehran, Iran.

Alireza Tehranian

Department of Biomedical Engineering, Faculty of Paramedical Sciences, Tehran Medical Sciences, Islamic Azad University, Tehran, Iran.

Ramin Ardalani

Department of Biomedical Engineering, Faculty of Paramedical Sciences, Tehran Medical Sciences, Islamic Azad University, Tehran, Iran.

Abstract

The increase in vertebral diseases has led to improvements in surgical operations and therefore implants. Due to the sensitive nature of the spinal cord, the treatment in this region has significant medical concerns and the properties of the implant used in this area are critical. It must have special mechanical and biological characteristics that are similar to those of bone. Nitinol is more suitable for orthopedic implants than other alloys because of its features such as super-elasticity, close-to-bone elastic modulus, and also its good biocompatibility. In this study, a lumbar vertebral implant was manufactured by a two-step processing method including sintering rod fabrication procedure and braiding technique and the effect of adding the braid to the structure was evaluated. The applied Scanning Electron Microscopy showed an average pore size of 310 micrometers in samples. The results of Atomic Force Microscopy demonstrated that the average roughness is 971.1 nm. The development of this type of implant aims to facilitate the treatment of vertebral areas.

Keywords: Vertebral implant, Nitinol, Biocompatibility

1- Introduction

The structural composition of the spine is characterized by its robustness since it serves the crucial function of safeguarding the spinal cord and spinal nerve roots [1]. Its favorable mechanical qualities and high fracture toughness enable it to facilitate motion and safeguard delicate inside organs [2]. The lumbar area, including various components such as visceral organs, has been identified as a potential origin of low back pain (LBP). The application of mechanical loads on the lumbar spine, together with the presence of inflammatory alterations, is contributing factors to the development of LBP [3]. LBP is characterized by the presence of discomfort that originates from the buttock region and thereafter travels down the trajectory of the sciatic nerve [4, 5]. In the last twenty-five years, there has been a notable rise in the occurrence of LBP [6]. The worldwide incidence of LBP was recorded to be 568.4 million cases around the world [7]. The treatment and healthcare of back pain have considerable financial and medical obstacles due to the delicate and vulnerable nature of the spinal cord [8]. Over the last two decades, significant researches have been undertaken to evaluate different materials for bone replacement, to provide substitutes for bone. It has been observed that materials falling within this category often include bioactive ceramics, biological or synthetic polymers, and it is more practical to fabricate orthopedic implants with metal alloys that exhibit exceptional mechanical properties [9, 10, 11, 12]. Spinal implants need the possession of two crucial attributes: mechanical qualities, including bio-functionality, and biological traits, including bio-compatibility. Among other alloys, nitinol has been chosen for orthopedic implants because it can go through a phase change called the martensite-austenite transformation which affects the mechanical properties of an implant to be near to bone. The commencement of this transition is often prompted by stimuli linked to temperature and/or stress [13]. Nitinol refers to a group of intermetallic materials mostly composed of titanium and nickel in about equal proportions. The shape memory and super elastic capabilities of Nitinol are attributed to its thermoelastic martensitic transition [14, 15, 16]. Nitinol has a diverse range of beneficial features, making it a very promising material.

On the other hand, owing to the invasiveness of surgery, bone tissue engineering (BTE) has become a potential bone regeneration strategy. Synthetic extracellular matrix (ECM) and osteogenic activity stimulate bone regeneration [17]. Ravindran et.al has shown that ECM ranks as the fourth most significant element in the development of BTE [18]. Therefore, the induction of osteogenic activity has been shown to enhance the process of bone regeneration [19, 20]. However, a porous structure within these structures allows materials to infiltrate into host tissue, stimulating cellular proliferation, capillary development, and bone tissue creation [21, 22, 23].

The issue of developing NiTi implants for lumbar vertebrae is a substantial challenge in the realm of orthopedic biomedical engineering, hence requiring more improvements. Nitinol is selected as the preferred material for the aforementioned application because of its superior performance features and given requirements. The current study used the sintering and braiding techniques simultaneously to make a nitinol implant in the shape of a lumbar vertebra. To achieve the construction of a framework that has both flexibility and endurance, the use of Nitinol wire necessitates the intricate interlacing of several strands. The use of the novel braiding method is distinguished by its simplicity and cost-effectiveness, rendering it an innovative and pragmatic approach to the production of this particular product. This methodology enables precise manipulation of the dimensions and configuration of the implant, making it appropriate for the fabrication of implants. The use of braiding methods enables the production of personalized implants that demonstrate improved mechanical and biological characteristics. It is important to note that using the rod without braid (WOB) would increase the shielding stress effect risk, which would make it less biocompatible and less likely to stick to things, which would reduce their overall benefits [24]. However, the absence of a rod would lead to unfavorable mechanical corrosion outcomes. A two-step approach was used, including the first fabrication of a rod, followed by the second procedure of wire encircling the aforementioned rod. The main aim of this work is to enhance the orthopedic biomedical engineering field through a meticulous investigation of the potential suitability of nitinol as a material for vertebral implants. This research is to augment orthopedic technology by a thorough examination of the potential applications of nitinol as a material for implants. Also, the present work introduces a novel production concept for nitinol, intending to facilitate more comprehensive investigations in this domain.

2- Experimental

2-1- Preparation process

The elements required to achieve a titanium concentration of 50.0% with nickel. It is noteworthy to state that a porosity maker was included to augment the porosity level to 50.0%, as shown in Table 1. Nitinol wire from the Baoji Hanz company was employed for this experiment, and its diameter was 0.25 mm. Urea's size showed a wide range of variability, from 100 to 600 μm . A pressure of 150 MPa was applied to the mixture. The specimen spent two hours undergoing thermal treatment in an argon-filled furnace at a temperature of 1050°C. Urea will be eliminated through evaporation, whereas titanium hydride will undergo decomposition, when the temperature reaches 200 and 500°C, respectively. It is important to mention that the material was exposed to both temperatures for one hour. The resulting sample measures 7 mm in height and 5 mm in diameter without the braid (WOB). In the next step, for obtaining samples with braid (WB), employing a machine for the braiding process proved to be immensely efficient in terms of time. The dimensions of the specimen were used to create a pattern, which was then woven together and placed in a cylinder around its circumference. Figures 1 and 2 show images of the finalized examples. Pair of wires was used to produce this texture. The rod (WOB) serves as the primary focus of the structure. As can be seen in Figure 1, the first wire makes its way down from the green area. After that, it leaves the green zone, with the "+" sign denoting the outside and the "-" symbol on the inside. This texture was produced by using two wires. The rod makes up the design's focal point. As shown in Figure 1, the first cable enters the underground zone in the green area, and then travels via green area 2, and so on until it emerges in green area 5. Next, the wire goes through a similar process inside the blue areas, but in reverse. Red lines on the rod indicate the exact points where two wires cross each other. Figure 2 shows the braided pattern without the rod. It's crucial to remember that this method was developed to improve mechanical and biological behavior. The presence of a braided cover helps biological properties and minimizing the use of Nitinol wire to the greatest extent possible proved to be a cost-effective approach while maintaining optimal performance. The following sections will provide a comprehensive account of the procedures involved in the development and production of the braid. Collaboration is advantageous and valuable in terms of fostering cooperation.

TABLE 1: PROVIDED FROM MERCK THE UREA, TITANIUM HYDRIDE, AND NICKEL POWDER.

Material	Purity	Particle size
Nickel Powder	99.9 %	$\leq 10 \mu\text{m}$
Titanium Hydride	99.5 %	$\leq 50 \mu\text{m}$
Urea	99.5 %	100-600 μm

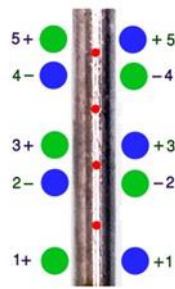


FIGURE 1: THE PLACE WHERE THE WIRES PASS THROUGH THE GREEN AND BLUE CIRCLES AROUND THE CYLINDER.



FIGURE 2: THE COVER AFTER THE PROCESS OF FIGURE 1.

2-2- SEM Image Analysis

The scanning electron microscope (SERON TECHNOLOGY, AIS2100, Korea) was used to analyze the surface morphology of the polished nitinol sample. In the processing method, Urea was added as a porosity maker to oblige the sample to be more compatible with the body in terms of stress shielding and cell adhesion. As every sample exhibits non-uniform surface conditions that are defined by features resembling dimples, the polishing procedure was applied. Then the sample undergoes a gold coating process using a technology that applies a 20 nm thick layer of gold by Physical Vapor Technology (PVD). The Nitinol specimen was examined using Digimizer 6 software to evaluate the pore size and its competence with the desired employment.

2-3- The AFM Test

In this phase, an experimental evaluation was conducted on WB and WOB samples to assess the surface roughness. The experiment was conducted using an Atomic Force Microscopy (AFM) apparatus manufactured by JPK business, specifically the Nanowizard 3 model. The first picture was captured using the non-contact imaging mode, resulting in a size of 10×10 micrometers and a resolution of 128 dots per inch (dpi). The subsequent region was chosen inside the first picture, measuring $1 \times 1 \mu\text{m}$, and was then captured at a resolution of 256 dots per inch (dpi). The analysis was performed with JPK Data Processing (version 5.0.96) and two-dimensional, three-dimensional images and their histogram frequency chart were presented in Figure 3 (a and b). The average surface roughness (Ra), the root means square roughness (RMS), and peak-to-valley roughness (Rt) are obtained by the software as indicated in Table 2.

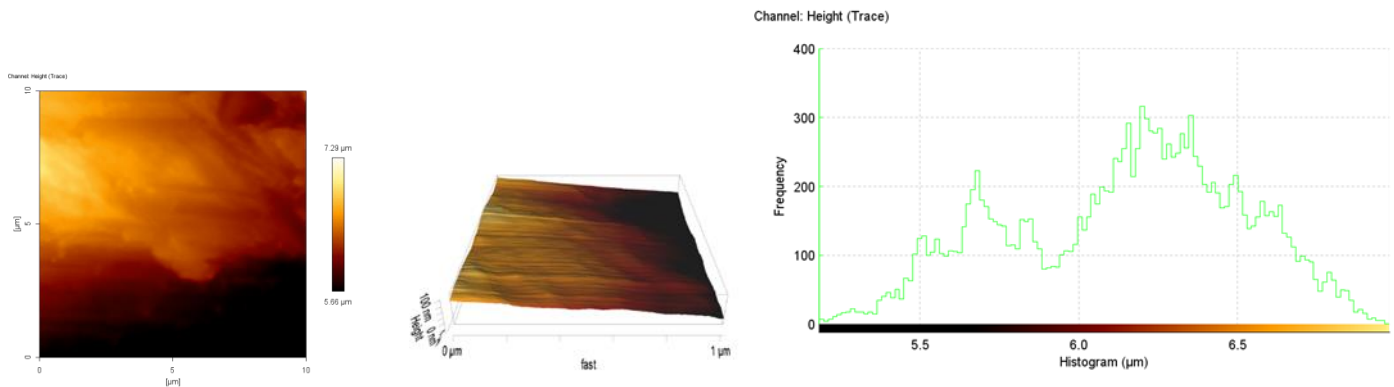


FIGURE 3a: 2D AND 3D AFM IMAGING AND HEIGHT HISTOGRAM OF NiTi BEFORE BRAIDING (WOB).

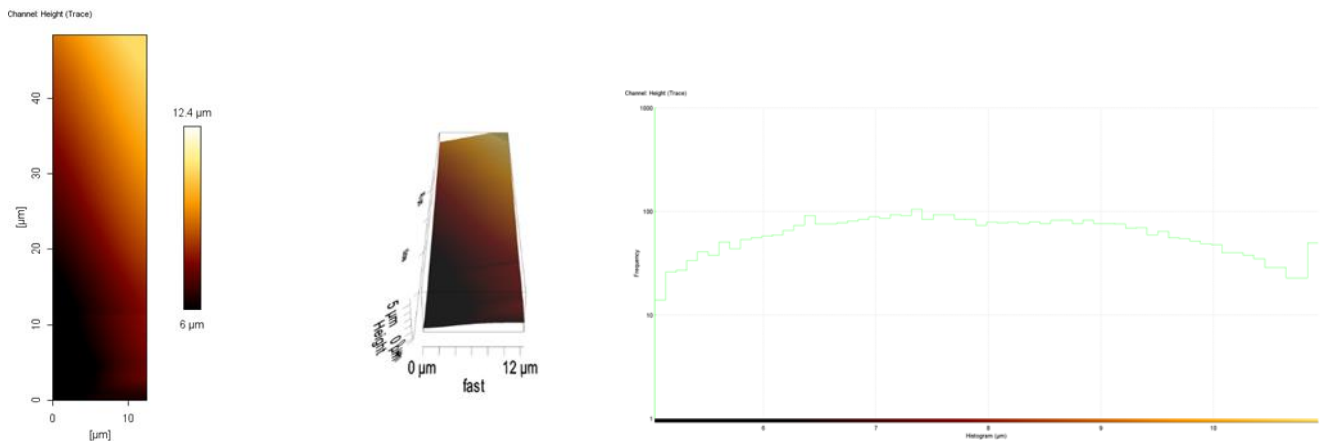


FIGURE 3b: 2D AND 3D AFM IMAGING AND HEIGHT HISTOGRAM OF NiTi AFTER BRAIDING (WB).

TABLE 2: NiTi ROUGHNESS INFORMATION WB AND WOB.

Roughness Information	A) Height (WOB)	B) Height (WB)
Average Value	6.144 μm	7.907 μm
Average Roughness Ra	267.5 nm	975.1 nm
RMS Roughness Rq	370.6 nm	1.433 μm
Peak-to-Valley Roughness Rt	1.782 μm	5.803 μm

3- Results and Discussion

3-1- Morphology Study

Figure 4 illustrates the SEM photographs of the materials. Table 3 provides details on the parameters of the pores, such as their length, perimeter, and area. The significance of pore size concerning cell development is well-established. When the pore size is small, cells have limitations in their ability to migrate towards the central region of a structure. This, in turn, hampers the diffusion of nutrients and the elimination of waste materials. On the other hand, if the pores exhibit excessive size, there is a resultant decrease in the specific surface area, hence imposing constraints on the attachment of cells. By choosing two pores in different magnifications and calculating with Digimizer 6 software, the average pore size observed in the sample is around 310 micrometers that indicated by the area of 48636.3142 square micrometers that by comparing this size with the size of pores in the bone [25] it can be demonstrated that the congruity between these two amounts is the preference of an orthopedic implant to have osseointegration and elimination of stress shielding. According to study [26], the best pore size for bone growth is 300-800 micrometers, which specifies the manufactured sample's suitability as a bone implant. This particular pore size has been shown to facilitate the optimal proliferation of bone cells and their adhesion [27, 28]. As a fact, cell adhesion plays a role in various natural processes, including maintaining tissue structure, healing wounds, and integrating biological materials into tissues. The biocompatibility of biomaterials is intricately related to the interaction between cells and the surface of the material, especially in terms of cell adhesion. Surface properties of materials, including their topography, are important factors in determining the adhesion of osteoblasts to biomaterials. This feature also affects bone cells [29], which can be seen in biological SEM images (Fig. 7). While there may be different forms in the behavior of diverse cells, it can be generally said that an appropriate sample will be available to support and facilitate bone cell activities in which the result of the applied biological tests also confirms the established pores in the samples coincide with

its application as an implant in hard tissue and caused cell mobilization. So, adding the Urea as a porosity maker does its work in the desired way for enhancing biological properties.

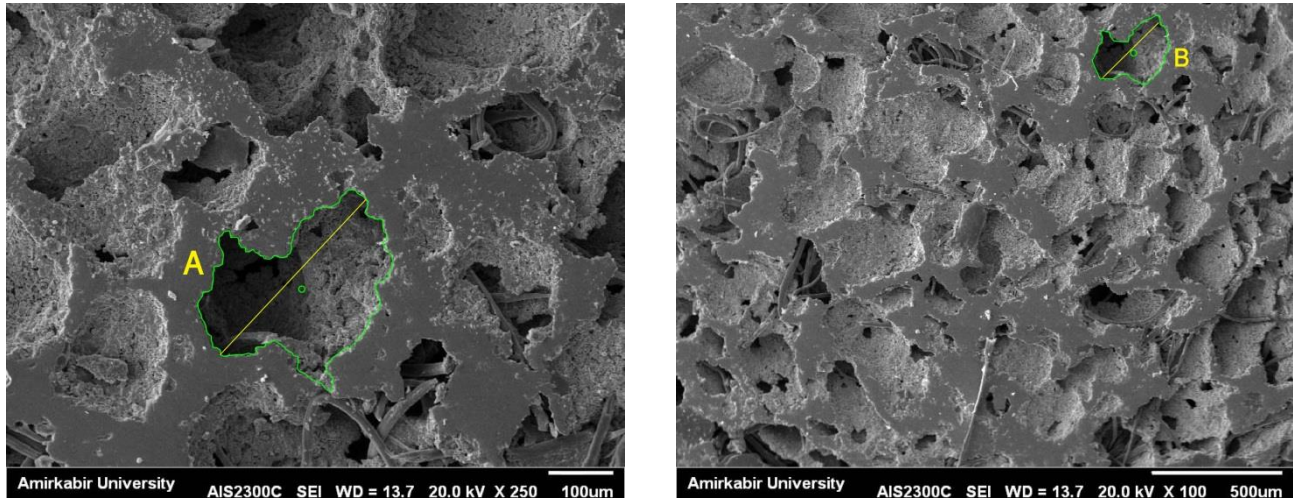


FIGURE 4: THE SEM IMAGES TAKEN AT TWO DIFFERENT MAGNIFICATIONS (A: 100 μm AND B: 500 μm).

TABLE 3: SPECIFICS OF THE PORE PARAMETERS, INCLUDING LENGTH, AREA AND PERIMETER.

	Length	Perimeter	Area
A (100 μm)	321.629 μm	1150.7824 μm	49382.4188 μm^2
B (500 μm)	300.126 μm	1006.9116 μm	47890.2095 μm^2
Mean	310.8775 μm	1078.847 μm	48636.3142 μm^2

3-2- AFM Result

The information about roughness is succinctly presented in Table 2. The average roughness for sample WB and WOB is 267.5 nm and 975.1 nm respectively ($p < 0.05$). By comparing these numbers, a significant increase in the roughness value was observed by appending the braid to the cylinder. Mainly by comparing the table amounts, the surface roughness becomes greater in WB. The AFM topography images and histogram of WOB and WB samples are assessed (Fig. 3a and 3b) to evaluate the nanodomain dimensions. The objective of this study is to optimize protein adsorption and cell adhesion, making this issue of utmost importance that the rise in roughness results in better cell adhesion (SEM images in Figure 7 confirm). To modify the rate of coagulability and enhance the prompt synthesis of cells and tissues, it is necessary to make modest adjustments to the porosity and roughness. As roughness is a notable factor needed for the manufacturing of metal implants that affects bone integration, by investigating the results achieved from this test and SEM analysis, it can be stated that the feature in the samples with braid can be suitable for implementation in the bone area.

4- Conclusion

In this research, the sample was manufactured by a two-step process including rod fabrication and braiding technique, and the effect of this braid was evaluated. In the SEM images, the pore size of approximately 310

micrometers was reported which is a suitable size for bone tissue engineering. The results of AFM illustrated that the amount of roughness changed to an acceptable amount and its average (Ra) is 971.1 nm which provides good conditions for bone cells. It can be concluded that adding a braid to the structure improves its preference as a vertebral implant.

References

- [1] Allegri M, Montella S, Salici F, Valente A, Marchesini M, Compagnone C, Baciarello M, Manferdini ME, Fanelli G. Mechanisms of low back pain: a guide for diagnosis and therapy. F1000Research. 2016;5.
- [2] Stevens MM. Biomaterials for bone tissue engineering. Materials today. 2008 May 1;11(5):18-25.
- [3] Shin SW. Low back pain: review of anatomy and pathophysiology. Journal of the Korean Medical Association. 2006 Aug 1;49(8):656-64.
- [4] Vlaeyen, J.W.S., Maher, C.G., Wiech, K. et al. Low back pain. Nat Rev Dis Primers 4, 52 (2018).
- [5] Urits I, Burshtein A, Sharma M, Testa L, Gold PA, Orhurhu V, Viswanath O, Jones MR, Sidransky MA, Spektor B, Kaye AD. Low back pain, a comprehensive review: pathophysiology, diagnosis, and treatment. Current pain and headache reports. 2019 Mar; 23:1-0.
- [6] Hurwitz EL, Randhawa K, Yu H, Côté P, Haldeman S. The Global Spine Care Initiative: a summary of the global burden of low back and neck pain studies. European Spine Journal. 2018 Sep; 27:796-801.
- [7] Chen S, Chen M, Wu X, Lin S, Tao C, Cao H, Shao Z, Xiao G. Global, regional and national burden of low back pain 1990–2019: a systematic analysis of the Global Burden of Disease study 2019. Journal of orthopaedic translation. 2022 Jan 1; 32:49-58.
- [8] Wolman DN, Heit JJ. Recent advances in vertebral augmentation for the treatment of vertebral body compression fractures. Current Physical Medicine and Rehabilitation Reports. 2017 Dec; 5:161-74.
- [9] Kok D, Donk RD, Wapstra FH, Veldhuizen AG. The memory metal minimal access cage: a new concept in lumbar interbody fusion—a prospective, noncomparative study to evaluate the safety and performance. Advances in Orthopedics. 2012 Jan 1;2012.
- [10] Litak J, Szymoniuk M, Czyżewski W, Hoffman Z, Litak J, Sakwa L, Kamieniak P. Metallic implants used in lumbar interbody fusion. Materials. 2022 May 20;15(10):3650.
- [11] Hench LL, Polak JM. Third-generation biomedical materials. Science. 2002 Feb 8;295(5557):1014-7.
- [12] Liu CZ, Czernuszka JT. Development of biodegradable scaffolds for tissue engineering: a perspective on emerging technology. Materials science and technology. 2007 Apr 1;23(4):379-91.
- [13] Pincus T, Vlaeyen JW, Kendall NA, Von Korff MR, Kalauokalani DA, Reis S. Cognitive-behavioral therapy and psychosocial factors in low back pain: directions for the future. Spine. 2002 Mar 1;27(5):E133-8.
- [14] Otsuka K, Wayman CM, editors. Shape memory materials. Cambridge university press; 1999 Oct 7.
- [15] Porter DA, Easterling KE. Phase transformations in metals and alloys, 2nd Editio.
- [16] Saigal A, Fonte M. Solid, shape recovered “bulk” Nitinol: Part I—Tension–compression asymmetry. Materials Science and Engineering: A. 2011 Jun 25;528(16-17):5536-50.
- [17] Parsafar M, Sadrnezhad SK, Nemati NH. Design and preparation of nickel-titanium implant for lumbar vertebra. Journal of Alloys and Compounds. 2023 Mar 5;936:167969.
- [18] Ravindran S, Gao Q, Kotecha M, Magin RL, Karol S, Bedran-Russo A, George A. Biomimetic extracellular matrix-incorporated scaffold induces osteogenic gene expression in human marrow stromal cells. Tissue Engineering Part A. 2012 Feb 1;18(3-4):295-309.

- [19] Ghanbari M, Salavati-Niasari M, Mohandes F. Injectable hydrogels based on oxidized alginate-gelatin reinforced by carbon nitride quantum dots for tissue engineering. *International Journal of Pharmaceutics*. 2021 Jun 1;602:120660.
- [20] Livingston TL. Bioactive scaffold for bone tissue engineering: An in vivo study. University of Pennsylvania; 1999.
- [21] Abbasi N, Hamlet S, Love RM, Nguyen NT. Porous scaffolds for bone regeneration. *Journal of science: advanced materials and devices*. 2020 Mar 1;5(1):1-9.
- [22] Oliveira JD, Aguiar PD, Rossi AM, Soares GA. Effect of process parameters on the characteristics of porous calcium phosphate ceramics for bone tissue scaffolds. *Artificial organs*. 2003 May;27(5):406-11.
- [23] Wen CE, Yamada Y, Shimojima K, Chino Y, Hosokawa H, Mabuchi M. Novel titanium foam for bone tissue engineering. *Journal of materials research*. 2002 Oct;17:2633-9.
- [24] Taheri Andani M, Haberland C, Walker JM, Karamooz M, Sadi Turabi A, Saedi S, Rahmanian R, Karaca H, Dean D, Kadkhodaei M, Elahinia M. Achieving biocompatible stiffness in NiTi through additive manufacturing. *Journal of Intelligent Material Systems and Structures*. 2016 Nov;27(19):2661-71.
- [25] Yamahara S, Raudales JL, Akiyama Y, Ito M, Chimedtseren I, Arai Y, Wakita T, Hiratsuka T, Miyazawa K, Goto S, Honda M. Appropriate pore size for bone formation potential of porous collagen type I-based recombinant peptide. *Regenerative Therapy*. 2022 Dec 1;21:294-306.
- [26] Murphy CM, O'Brien FJ. Understanding the effect of mean pore size on cell activity in collagen-glycosaminoglycan scaffolds. *Cell adhesion & migration*. 2010 Jul 1;4(3):377-81.
- [27] Kuboki Y, Jin Q, Takita H. Geometry of carriers controlling phenotypic expression in BMP-induced osteogenesis and chondrogenesis. *JBJS*. 2001 Apr 1;83(1):S105-15.
- [28] Tsuruga E, Takita H, Itoh H, Wakisaka Y, Kuboki Y. Pore size of porous hydroxyapatite as the cell-substratum controls BMP-induced osteogenesis. *The Journal of Biochemistry*. 1997;121(2):317-24
- [29] Anselme K. Osteoblast adhesion on biomaterials. *Biomaterials*. 2000 Apr 1;21(7):667-81.